

A COMPARISON OF ELECTROMAGNETIC METHODS WITH THE DC RESISTIVITY MULTIPLE-SOURCE BIPOLE-DIPOLE METHOD FOR DEEP GEOTHERMAL EXPLORATION

T.G. CALDWELL AND H.M. BIBBY

Institute of Geological and Nuclear Sciences Ltd., Wellington

ABSTRACT - An evaluation of the utility of 4 different electromagnetic (EM) methods for exploration of the deeper parts of a geothermal reservoir was recently published by Pellerin *et al* (1992). The DC resistivity multiple-source bipole-dipole technique has been used successfully in NZ for the exploration of the deeper levels of the geothermal systems for many years. In this paper, results of a similar evaluation of the DC resistivity multiple-source bipole-dipole technique is presented and compared with the EM techniques. Using 3 dimensional (3D) numerical models the ability of each technique to detect the existence of an idealised geothermal reservoir beneath a highly conductive zone near the surface are compared. The Pellerin *et al.* study showed that, of the EM techniques, only the Magneto Telluric (MT) and Long Offset Time Domain EM (LOTEM) methods will detect the presence of the reservoir. 3D modelling shows that the DC technique will detect the deeper resource equally well. Indeed the electric field response from the LOTEM method at late times, where the response of the reservoir is seen, is identical to the DC resistivity response.

INTRODUCTION

Over the last 10 years the ability to numerically model the electromagnetic (EM) response of 3 dimensional (3D) resistivity distributions has improved markedly (Wannamaker 1991, Newman *et al.* 1986, Druskin and Knizherman 1988). Recently, Pellerin *et al.* (1992) used a number of these techniques to conduct an evaluation of EM exploration methods for geothermal exploration. In particular magneto telluric (MT), controlled source audio-frequency magneto telluric (CSAMT), time domain EM sounding (TEM) and long offset time domain electromagnetic (LOTEM) methods were tested. Each technique was applied to a standard model to test the ability to detect the presence (or otherwise) of a low resistivity prism beneath a shallow highly conductive zone. The 3D resistivity model used by Pellerin *et al.* (1992) and in this paper to represent the geothermal system is shown in Figure 1. The highly conductive zone, $5 \Omega\text{m}$ in the models, represents the smectite-illite clay alteration zone that often occurs at the upper levels of a high temperature geothermal system (Simmons and Browne, 1990). The underlying high temperature geothermal reservoir is represented by a $25 \Omega\text{m}$ prism extending beneath the $5 \Omega\text{m}$ zone to a depth of more than 5 km. Background resistivity is taken to be $200 \Omega\text{m}$. In addition to the block model, an axially symmetric model, shown in Figure 2, was also used for the study of the DC response.

The resistivity model used in the EM study was designed by Pellerin *et al.* (1992) in conjunction with scientists from the geothermal division of Unocal. There is general agreement between this model and the model of the Ohaaki geothermal

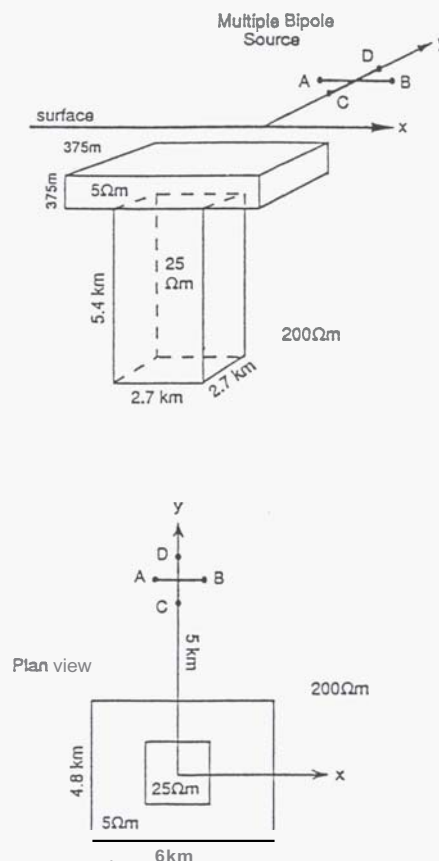


Figure 1: Resistivity model used for integral equation calculation of DC apparent resistivity. This model is same as that used by Pellerin *et al.* (1992) for the EM calculations discussed in the text.

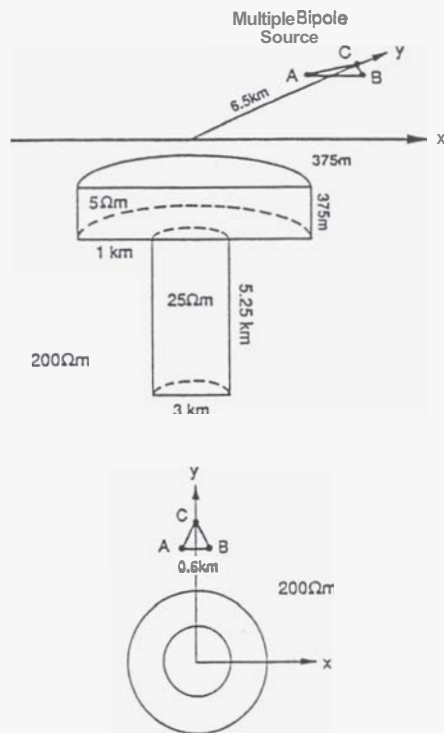


Figure 2: Resistivity model used for axially symmetric finite element calculations. The axially symmetric model used has diameters equal in length to the widths (along the y axis) of the rectangular bodies used for the models shown in Fig 1.

system derived from bipole-dipole DC resistivity data by Bibby and Risk (1973) and Bibby (1978). In particular, the large near surface resistivity contrast and the increase of the resistivity with depth within the geothermal field are features that have been detected at Ohaaki. The results of the EM modelling study suggest that all the techniques can delineate the clay cap, but only the MT and LOTEM electric field techniques produce a response from the deeper body large enough to identify a reservoir underlying a surficial alteration zone.

The purpose of this paper is to present the results of a similar set of model calculations for the DC resistivity multiple-source bipole-dipole technique. This DC method has been the main tool used in New Zealand for the geophysical exploration of the deeper parts of the geothermal systems in the Taupo Volcanic Zone (TVZ), (Bibby and Risk, 1973, Bibby *et al.* 1984, Risk *et al.* 1984) and more recently for studies of the large Scale resistivity study of the TVZ, (Risk *et al.*, in press).

MULTIPLE-SOURCE BIPOLE-DIPOLE METHOD

The geometry of the multiple-source bipole-dipole array as typically used by for geothermal exploration in New Zealand is shown in Figure 3. Current is injected sequentially into the 3 bipoles formed from pairs of three current electrodes. Electric fields due to each bipole are measured at a remote point P using two approximately perpendicular dipoles. Typically these dipoles are 50m long

while the current electrodes are separated by a 2 or 3 km. More details on the equipment and field procedure used in recent surveys in NZ maybe found in Risk *et al.* (in press).

The advantage of the multiple-source bipole-dipole technique lies in the ability to represent the resulting apparent resistivity in the form of a tensor (Bibby 1977, 1986). In particular, if the total field apparent resistivity produced by each bipole source (Bibby and Risk, 1973) is plotted in the direction of the corresponding electric field vector, as shown in Figure 3, then it can be shown that their tips will lie on an ellipse. That is, the ellipse is graphical representation of the tensor relationship between the current densities present in a uniform half space and the measured electric fields (Bibby 1977, 1986). For any measurement site there are 3 co-ordinate invariant properties of the ellipse that may be used to map the apparent resistivity. For

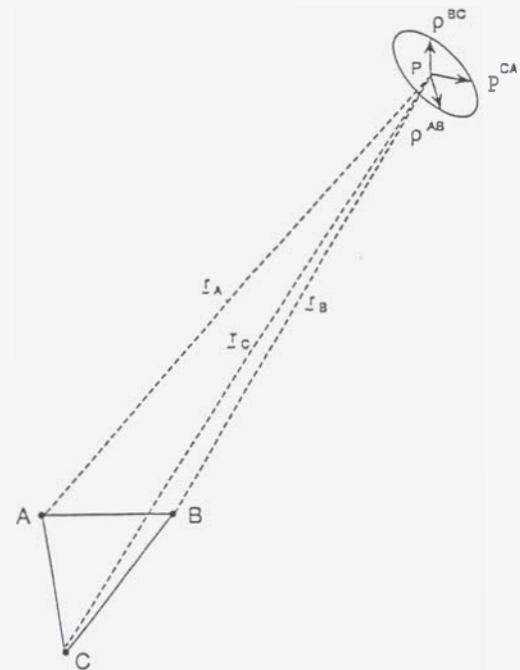


Figure 3: Geometry of multiple-source bipole-dipole array. Electric field measurements from each bipole can be combined to define an apparent resistivity tensor which can be represented graphically by an ellipse. The apparent resistivity P_2 used later in this paper is given by the geometric average of the principal axes of the ellipse.

example, the area of the ellipse obviously does not depend on the reference frame used for the measurements. Furthermore, provided the distance of the measurement point is great enough, the invariants of the apparent resistivity tensor, and in particular the shape of the ellipses, are independent of the orientation of the source bipoles. The parameter denoted by P_2 which is used to show the model results is one such invariant, and can be shown to be related to the area of the ellipses. This co-ordinate invariant parameter, an apparent resistivity, has been shown to give a remarkably good picture of the resistivity distribution even

in quite complex 3D situations (Bibby and Hohmann, in press).

MODELLING METHOD

The model results presented here were calculated using both a 3D integral equation technique developed by Hohmann (1975) and an axially symmetric finite element technique developed by Bibby (1978). Figures 1 and 2 show the form of these models. The model used for the integral equation calculation (Figure 1) is the same as used by Pellerin *et al.* for the EM study. Using two different modelling schemes enabled us to verify that errors introduced into the results by the discretisation process are negligible. Also, as we will show later, the large effects that occur at the corners of the low resistivity blocks are absent from the axially symmetric models. Thus, the axially symmetric models provide a slightly more stringent test of the detectability of the underlying reservoir. Following Pellerin *et al.* (1992) the top of the 5 Ωm body is modelled as lying 375m below the surface. Although this may over estimate the depth at which low resistivity actually occur in a geothermal field this restriction is necessary to ensure that the calculation of the electric field at the surface are accurate near the resistivity boundaries of the 5 Ωm body. Similar precautions are evident in the model used for the EM calculations. The 3D model used for the DC modelling consisted of 228 prisms with the calculation taking about 13 minutes of CPU time on a VAX station 4000-60. The axially symmetric model consisting of 2500 elements took less than a minute of CPU time.

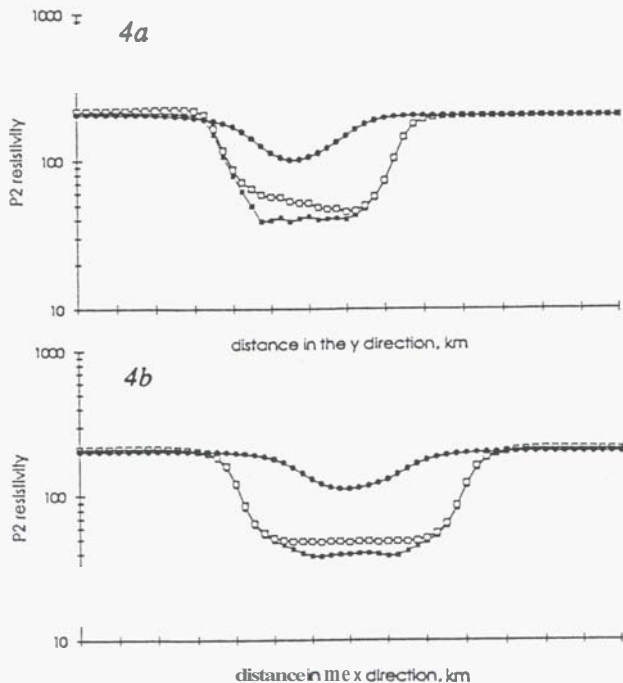


Figure 4: P2 apparent resistivity calculated along the y (Fig. 4a) and x (Fig. 4b) axes of the model shown in Fig. 1. The solid and open squares show the results calculated with and without the 25 Ωm body present, respectively. The filled circles show the apparent resistivity calculated for a model consisting of the 25 Ωm prism alone.

RESULTS

Figure 4 shows the apparent resistivity invariant P2 computed along the x and y axes for the model shown in Figure 1. The position of one of the current bipoles (AB) used in the calculations of these results is the same as that used by Pellerin *et al.* for their calculations of the CSAMT and LOTEM responses. The second bipole is of equal length, perpendicular to AB. Filled and open squares have been used to distinguish the results calculated with and without the 25 Ωm body. The filled circles show the response that would be observed over the 25 Ωm body in the absence of the upper conductive material. Similar graphs are shown for the axially symmetric model in Figure 5.

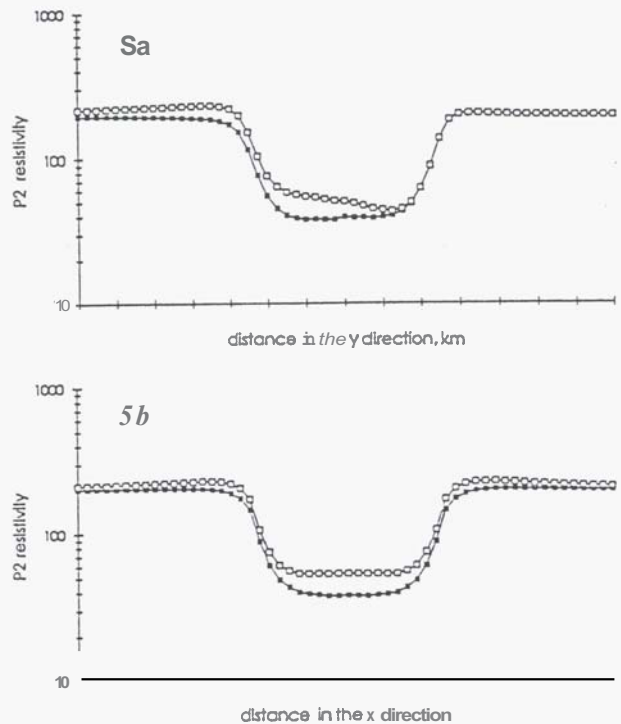


Figure 5: P2 apparent resistivity calculated along the x (Fig. 5a) and y (Fig. 5b) axes of the axially symmetric model shown in Fig. 2. The diameter of the axially symmetric model was chosen to be the same as the width in the x direction for the model shown in Figure 1. Solid and open symbols denote values calculated with and without 25 Ωm body respectively.

As expected all the profiles detect the 5 Ωm resistivity body, with a rapid fall in apparent resistivity accurately marking its extent. Profiles running away from the source (Figures 4a and 5a) retain some of the properties of a depth sounding even in this 3D situation. In the case, where only the near surface body is present, the influence of 200 Ωm material beneath the conductive zone causes the apparent resistivity over the body to increase with increasing source receiver separation. This behaviour can also be seen on the contour maps of apparent resistivity, given in Figures 6 and 7, which show the distribution of apparent resistivity for the 3D and axially symmetric models respectively.

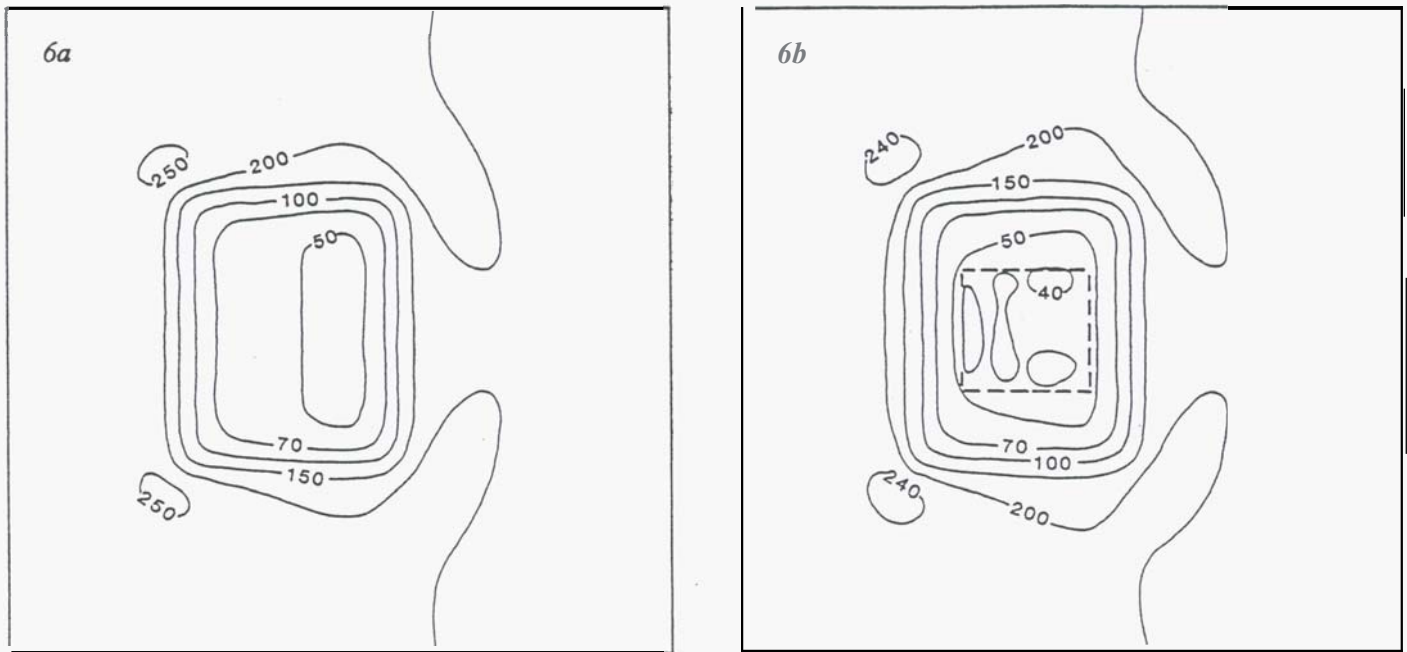


Figure 6: P2 apparent resistivity map for 3D model shown in Figure 1. The results for the case where only the $5 \Omega \text{ m}$ prism is present in the model is shown in Figure 6a. Figure 6b shows the results where both the $5 \Omega \text{ m}$ and $25 \Omega \text{ m}$ prisms are present.

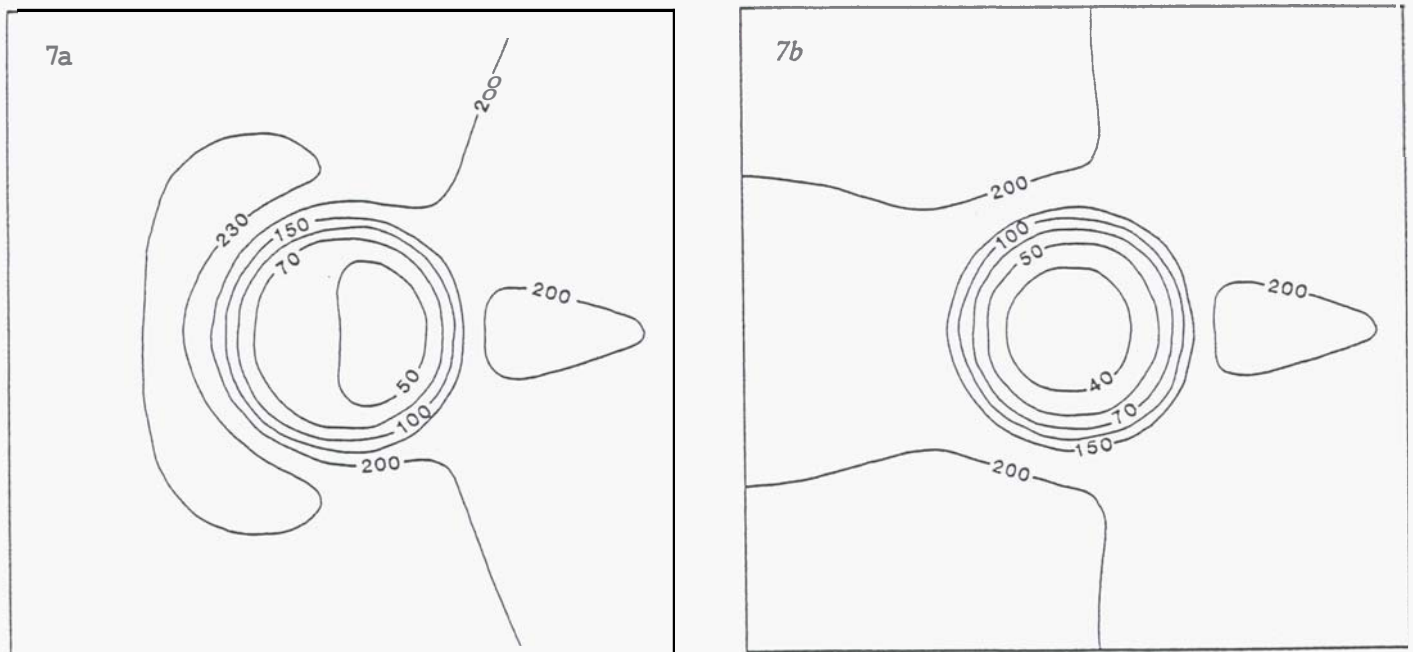


Figure 7: P2 apparent resistivity map for axially symmetric model shown in Figure 2. Figure 7a and 7b show the results for a model consisting of only the near surface $5 \Omega \text{ m}$ body and for a model including both $5 \Omega \text{ m}$ body and the $25 \Omega \text{ m}$ body representing the reservoir respectively

One notable difference between the axially symmetric and block models *can* be observed in these maps. Large apparent resistivity anomalies produced near the corners of the 5 Ωm prism *are* absent in the results from the axially symmetric model. These effects *are* not artefacts of the computation but a consequence of the geometry. Similar effects will *also* occur *at* the corners of the underlying 25 Ωm prism. The small apparent resistivity changes coinciding with edges of the 25 Ωm prism, most obvious in Figure 4b, appear *to be* a result these effects. Such extreme geometry is unlikely to occur in practice and the axially symmetric results are thus regarded *as giving* a more realistic picture of the response.

Including the 25 Ωm body in the models completely changes the aspect ratio of the conductive mass. When the deeper body is absent increasing the source receiver separation increases the influence of the high resistivity beneath the surface layer, and thus increases the apparent resistivity. With lower resistivity at depth, this affect is not observed. This suggests that the response observed at the surface is dominated by 3B effects, that is by effects produced by the lateral boundaries. Adding the 25 Ωm body to the model reduces the apparent resistivity by up to 30%. Values within the low resistivity area are about 40 Ωm and remain approximately constant over the 5 Ωm resistivity body.

These results indicate that the lateral boundaries of the shallow conductive body produce the largest part of the response. The boundaries of the 25 Ωm prism *will* also produce significant effects *as can be seen* (Figure 4) in the response due to the 25 Ωm body alone. Despite the depth of burial (750m) this body produces a 50% decrease in apparent resistivity from background with the low resistivity anomaly centred almost exactly over the 25 Ωm prism.

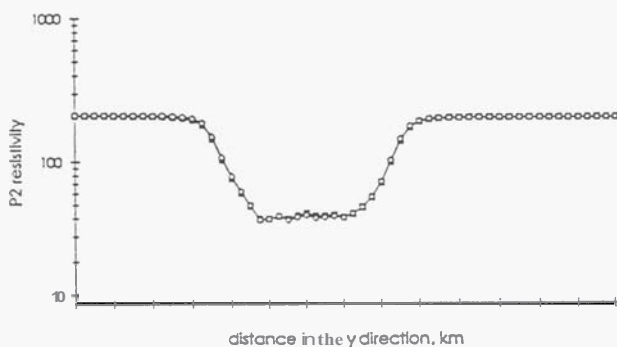


Figure 8: A profile of the P2 apparent resistivity calculated with a source sited 10.5km from the centre of the model is shown as open squares. The filled squares are the results also shown in figure 4 for a source 3km closer to the centre of the model.

It is interesting to ask whether increasing the distance between the source and model would significantly increase the response from the deeper body. Figure 8 shows the results of calculations made with source bipoles placed 3km

further away from the model. The apparent resistivity response produced in this case is virtually identical to results calculated with the closer source confirming the importance of the lateral boundaries. The response of the bipole-dipole method is a measure of the distortion of the electric compared with the field expected in a uniform half space. These distortions can be viewed as an effect of charge accumulations at the resistivity boundaries and can be thought of as a capacitive effect.

COMPARISON WITH OTHER TECHNIQUES

Like the DC bipole-dipole technique the CSAMT method uses a grounded current bipole as a signal source. However, rather than determining the relationship between a theoretical current density and measured electric field the CSAMT method measures the electric and magnetic fields over a broad range of source frequencies at points remote from the source. The relationship between these fields is used to define an apparent resistivity. Identical measurements are used in MT method, the difference between the CSAMT and MT methods being the MT methods use natural fluctuations in the earth's magnetic field as a signal source. In principle the depth of investigation of these two methods is determined by the frequency of the EM field; the longer the period the greater the detection depth.

Simple skin depth criteria for an EM plane wave incident onto a conducting body suggest that signals with periods greater than about 1 second should be capable of detecting the 25 Ωm prism. The MT model calculations confirm this, although, as Pellerin *et al.* (1992) show, the dominant component of the response is, like the bipole-dipole response, due to boundary charges. In other words, the signal is in the electric field component, rather than in the magnetic field. Pellerin *et al.* (1992) conclude that "MT shows a modest reservoir anomaly that may be measurable, but requires multi-dimensional interpretation."

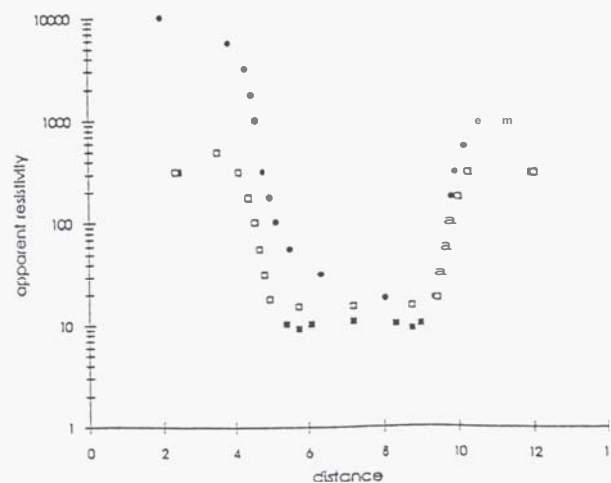


Figure 9 Profiles showing the MT and CSAMT apparent resistivity (1Hz) as calculated by Pellerin *et al.* (1992).

Only the CSAMT results for the model including both conductive prisms were published by Pellerin *et al.* (1992)

These results and the corresponding MT apparent resistivity **are** shown in Figure 9. **As** noted by Pellerin *et al.*, the plane wave assumption that is made in the calculation and interpretation of **CSAMT** results is not valid at the frequencies *required* to detect the body. The difference between the MT and CSAMT apparent resistivity in Figure 9 is a consequence of **this** problem. To ensure plane waves at a period of **1** second would *require* moving the source bipole to a distance of at least 20km from the model. At these distances the magnetic field strength is very small making reliable **data** collection very difficult. **Thus**, in its present form the **CSAMT** method is unlikely to provide a useful tool for exploring the deeper parts of a geothermal **system**. However, it is important emphasise that the difficulties are a consequence of the plane wave assumption used in the analysis. As is demonstrated by the MT **results** effects from the deeper body must also be present in the long **period** CSAMT **data**.

The current sources used for LOTEM and DC resistivity bipole-dipole surveys are essentially identical. Both methods **use** a very long **period** square wave **as** the current waveform. The transient EM field produced by the leading and falling edges of this waveform provides the signal used in LOTEM measurements. For practical reasons it is **usual** to measure only the electric and vertical magnetic field transients (Strack 1992). The behaviour of the transient fields **as** a function of time is dependant on the resistivity distribution in the *earth*. In a simple layered situation detection depth will increase with increasing time. However, in a 3D situation with large resistivity contrasts boundary charge effects will dominate the response invalidating the relation between time and detection depth. At late times the LOTEM electric field response must asymptotically approach the DC electric field produced by the **source** bipole.

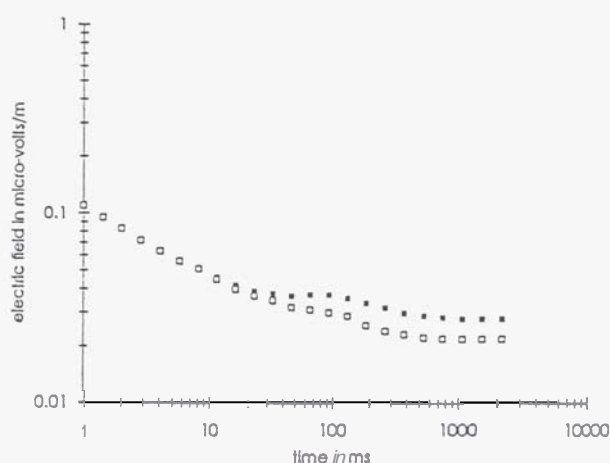


Figure 10 The transient electric field response measured with the WTEM techniques. Note that the electric field asymptotes to the DC response for the same model

Figure 10 shows the **LOTEM** electric field response calculated by Pellerin *et al.* (1992) for a point near the centre of the resistivity model shown in Figure 1. As the graphs show, the transient electric fields for both the model

with and without the deeper structure reach the DC electric field values after about **0.5s**. The signal due to the 25 Ωm body produced by the deep **reservoir** is first **seen** at about 30ms with the ratio between the two responses remaining constant after approximately **100ms** has elapsed. In contrast the vertical magnetic field response due **to** models with and without the 25 Ωm **prism** **are** indistinguishable (Pellerin *et al.* 1992).

CONCLUSIONS

In effect the bipole-dipole method measures effects of **boundary** charges only. **Thus**, for resistivity distributions where eddy current (inductive) effects **are** small compared with **boundary** charge effects the electric field **response** measured by the LOTEM or CSAMT methods **will** be well approximated by the bipole-dipole electric field **measured** with the bipole-dipole array.

Our modelling, using both 3D prism models similar to those **used** in the EM study and axially symmetric models, show that the apparent resistivity response of the DC resistivity technique is **as** great **as** the two EM methods (MT and LOTEM) that detect the model **reservoir** beneath a surficial conductive zone. Indeed, at late times the LOTEM electric field response must be the **same** **as** a single source resistivity bipole-dipole survey **as** the physical situation is identical. For the investigation of the deep electrical structures typical of geothermal systems, DC techniques will be **equally** effective **as** electromagnetic methods. Furthermore, DC techniques have the advantage that field operations **are** relatively simple and interpretation can **utilise** fast computer **algorithms**.

Using multiple-source DC **techniques**, combined with tensor apparent resistivity analysis makes **full** use of the information obtained with differently **oriented** current fields. Indeed better results may **be** obtained by combining the LOTEM system with the DC multiple-source technique. This **also** suggests that the development of tensor analysis techniques for multiple-source **LOTEM** surveys may provide similar advantages. Combined LOTEM and DC multiple-source techniques **are** being **used** by the Institute of Geological and Nuclear Sciences in the study of the deep electrical structure of the TVZ. As yet it is not clear to the authors whether or not the extra effort needed to collect and analyse both LOTEM and bipole-dipole data simultaneously is **justified** by the extra information gained.

ACKNOWLEDGMENTS:

We **would** like **to** thank staff at USGS, Branch of Geophysics in Denver for their hospitality during TGC's visit and in particular we would like to thank **Louise** Pellerin for stimulating **this** work.

REFERENCES:

Bibby, H.M., 1977: The apparent resistivity tensor. *Geophysics* 42,1258-1261.

Bibby, H.M., 1978: Direct current resistivity modeling for axially symmetric bodies using the finite element method. *Geophysics*, 4, 550-562.

Bibby, H.M., 1986: Analysis of multiple source bipole-quadrupole resistivity surveys using the apparent resistivity tensor. *Geophysics*, 51, 972-983.

Bibby, H.M., and Hohmann, G.W., in press: Three dimensional interpretation of multiple source bipole-dipole data using the apparent resistivity tensor. *Geophysical Prospecting*.

Bibby, H.M., Dawson, G.B., Raynor, H.H., Stagpoole, V.M. and Graham, D.J., 1984: The structure of the Mokai Geothermal Field based on geophysical observations. *J. Volcanology and Geothermal Res.*, 20, 1-20.

Bibby, H.M., and Risk, G.F. 1973: Interpretation of dipole-dipole resistivity surveys using a hemispheroidal model. *Geophysics* 38, 719-736.

Druskin, V.L., and Knizherman, L.A., 1988: A spectral semi-discrete method for the numerical solution of 3D nonstationary problems in electrical prospecting. *Physics of the Solid Earth*, 24, 63-74.

Hohmann, G.W., 1975: Three-dimensional induced polarization and electromagnetic modelling. *Geophysics*, 40, 309-324.

Newman, G.A., Hohmann, G.W. and Anderson, W.L., 1986: Transient electromagnetic response of a three dimensional model in a layered earth. *Geophysics*, 51, 691-706.

Pellerin, L., Johnston, J.M., and Hohmann, G.W., 1992: Evaluation of electromagnetic methods in geothermal exploration. Expanded Abstracts with Biographies, 1992 Technical Program, Society of Exploration Geophysicists Sixty-Second Annual International Meeting, New Orleans, 405-408.

Risk, G.F., Rayner, H.H., Stagpoole, V.M., Graham, D.J., Dawson, G.B., and Bennie, S.L., 1984: Electrical resistivity survey of the Wairakei Geothermal Field. Geophysics Division Report No. 200, DSIR, Wellington.

Risk, G.F., Bibby, H.M., and Caldwell, T.G. in press: DC resistivity mapping with the multiple-source bipole-dipole array in the central volcanic region, New Zealand. *J. Geomag. Geoelectr.*

Simmons, S.F. and Browne, P.R.L., 1992: A three dimensional model of the distribution of hydrothermal alteration minerals within the Broadlands-Ohaaki geothermal field: Proc. 12th New Zealand Geothermal Workshop, 25-30.

Strack K.M., 1992: A practical review of deep transient electromagnetic exploration. Elsevier, Amsterdam.

Wannamaker, P.E., 1991: Advances in three-dimensional modeling using integral equations. *Geophysics* 56, 1716-1728.